Journal of Dental Sciences (2019) 14, 119–125

Available online at www.sciencedirect.com

ScienceDirect

journal homepage: www.e-jds.com

Original Article

# Accuracy of cone beam computed tomography in measuring thicknesses of hard-tissue-mimicking material adjacent to different implant thread surfaces

Ching-Yu Yen [a,c,1], Po-Jan Kuo [b,1], Chi-Yu Lin [c,d], Nancy Nie-Shiuh Chang [e], Hsiang-Yin Hsiao [b], Yu-Tang Chin [f,g], Chi-Chun Tsai **[,h], Sheng-Yang Lee [c,d,h*]

[a] Department of Oral and Maxillofacial Surgery, Chi-Mei Medical Center, Tainan, Taiwan
[b] Department of Periodontology, School of Dentistry, National Defense Medical Center and Tri-Service General Hospital, Taipei, Taiwan
[c] School of Dentistry, College of Oral Medicine, Taipei Medical University, Taipei, Taiwan
[d] Center for Tooth of Bank and Dental Stem Cell Technology, Taipei Medical University, Taipei, Taiwan
[e] Department of Periodontology, Taipei Medical University, Taipei, Taiwan
[f] Taipei Cancer Center, Taipei Medical University, Taipei, Taiwan
[g] PhD Program for Cancer Biology and Drug Discovery, College of Medical Science and Technology, Taipei Medical University, Taipei, Taiwan
[h] Department of Dentistry, Wan-Fang Medical Center, Taipei Medical University, Taipei, Taiwan

Received 20 February 2019; Final revision received 25 April 2019
Available online 14 May 2019

**KEYWORDS**
Cone beam computed tomography;
Bone thickness;
Dental implant

**Abstract** *Background/purpose:* To evaluate the measurement accuracy of hard-tissue thicknesses adjacent to dental implants with different thread designs on images obtained from cone beam computed tomography (CBCT) using an *in vitro* model.
*Materials and methods:* On 4 × 13-mm implant, the neck of the implant was designed with micro-threads, and the apical part was covered by macro-threads; these implants were placed in a vinyl polysiloxane block that mimicked hard-tissue. Models were prepared with various thicknesses of 2.0, 1.0, 0.5 and 0.3 mm adjacent to the dental implant. Each model was scanned using CBCT, and the thickness of the cortical bone from the outer surface of the micro-threads and macro-threads were recorded. Ground sections were prepared, and the thickness was measured with electronic calipers as the gold standard (GS) measurement.

* Corresponding author. School of Dentistry, College of Oral Medicine, Taipei Medical University, 250 Wu-Hsing Street, Taipei 11031, Taiwan.
** Corresponding author.
*E-mail addresses:* Jimmy3886@yahoo.com.hk (C.-C. Tsai), seanlee@tmu.edu.tw (S.-Y. Lee).
[1] Both authors contributed equally to this study.

https://doi.org/10.1016/j.jds.2019.04.001

*Results:* CBCT measurements of the micro-thread surface were consistently underestimated compared to the GS measurement when the thickness of the hard-tissue-mimicking material was $\leq$1.0 mm. In comparison, CBCT measurements of the macro-thread surface closely approximated the standard measurement, except when the thickness of the hard-tissue-mimicking material was 0.3 mm. The mean percentage errors from the standard measurement for the 2.0-, 1.0-, 0.5-, and 0.3-mm thickness groups were 4.8%, 16.4%, 37.8%, and 92.6%, respectively, for the micro-thread group, and were 0.6%, 2.9%, 9.5%, and 40.8%, respectively, for the macro-thread group.

*Conclusion:* Within the limitations of this study, we conclude that CBCT may not produce sufficient resolution for thin sections of hard tissue-mimicking materials adjacent to micro-thread surfaces.


## Introduction

Peri-implant bone thickness is a key factor for obtaining reliable and long-term stability of dental implant. As it is known that once there is the presence of bony defect such as fenestration or dehiscence within the bony wall of dental implants may lead to an unfavorable mechanical and esthetic outcomes.[1,2]

Periapical radiograph, which provides a bidimensional image about distal and mesial aspects, is still considered the standard radiographic examination for implant treatment. However, the bone thickness and bone morphology in the buccal-lingual direction cannot be assessed.[3] The information can be obtained using cone-beam computed tomography (CBCT), which generates three-dimensional data. CBCT produced higher-resolution isotropic volumetric data with higher geometric accuracy at lower effective radiation dose than convectional computed tomography.[4] Despite the advantages of CBCT, there are also disadvantages associated with this technique. One of the most discussed problems concerns the metal artifacts which affect the acquired image quality especially in the head and neck area.[5,6]

Numerous studies have been focused on the accuracy of measurement of the peri-implant bone thickness adjacent to dental implants.[7–10] This is an important concept, as postoperative assessments of implant treatment and implant planning in areas adjacent to dense radio-opaque materials using CBCT techniques depend on the accuracy of this technique. However, there is a paucity of published literature on the accuracy of CBCT images with regard to the thread design of implant surfaces adjacent to dental implants. Furthermore, little is known about how the homogenous thickness of hard-tissue-mimicking material influences the accuracy. Therefore, the aim of this study was to evaluate measurements of the thickness of hard-tissue-mimicking materials adjacent to dental implants with two thread designs in CBCT using an *in vitro* model.

## Materials and methods

### Sample preparation and implant placement

In this study, vinyl polysiloxane (VPS) (Panasil® putty soft, kettenbach, Eschenburg, Germany) was selected and prepared as hard-tissue-mimicking material. Four blocks, approximately 30 × 20 × 15 mm, were made by using VPS. On the superior border of each block, two cylindrical holes were prepared. Using computed-assisted drilling, the distance between the holes was controlled to obtain different VPS thicknesses. The depth gauge ruler on the drill stand was set so that the site could be prepared two cylindrical holes with 4-mm diameter and 14-mm depth from the superior aspect of the block. After completion of drilling, a 4 × 13-mm implant (OsseoSpeed, Dentsply Astra implants, Mölndal, Sweden) was placed with a titanium healing cap. The neck of the implant was designed with micro-threads (0.22 mm), and the apical part was covered with macro-threads (0.66 mm). Each VPS block contained one implant and there were four VPS widths adjacent to the dental implants (2.0, 1.0, 0.5, and 0.3 mm) (Fig. 1).

### CBCT scanning

CBCT scanning was undertaken using a clinically available machine (i-CAT Next Generation®, Imaging Sciences International, Hatfield, PA, USA). A positional device with manufacturer-supplied quality assurance was used for secure attachment of VPS block. This provided an ideal horizontal platform and a reproducible position of the blocks relative to the CBCT machine. A laser orientation beam from the machine was used to aid alignment of the block so that the laser beam passed through the center of each block. A specialist dental radiologist performed all scans of the blocks.

The exposure settings selected were a 360° scan at 120 kV and 35 mA, with an acquisition time of 7.0 s. The scanning parameters were set to a field of view of 80 mm height and 80 mm width, a voxel size of 0.25 mm, a slice interval of 0.25 mm, and a slice thickness of 0.25 mm. A scout view was taken, and adjustments were made prior to final image acquisition to ensure correct alignment of the block. Following exposure, images were viewed independently and saved to DICOM files using i-CAT Vision software (Imaging Sciences International, Hatfield, PA, USA).

### CBCT image evaluation and measurement

The viewing software utilized to analyze the CBCT images was OsiriX MD (Pixmeo Sarl, Geneva, Swiss). For each implant, the image display was standardized to adjust the

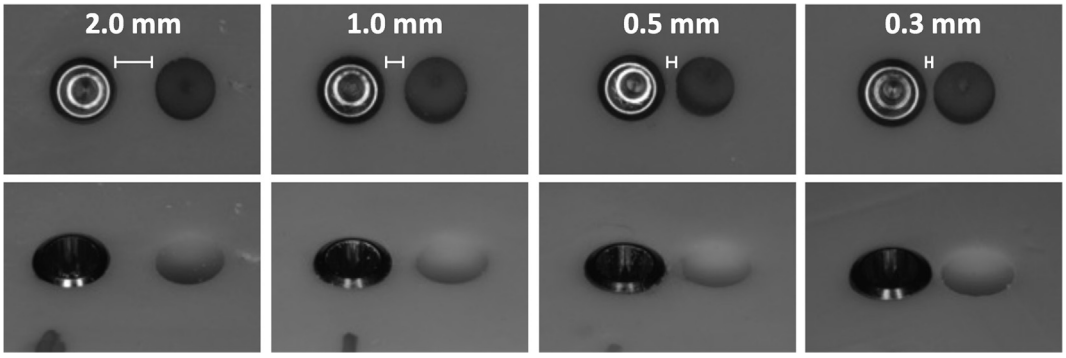


**Figure 1** Upper illustrations present of the 4.0 × 13 mm implants placed adjacent the cylindrical hole in the vinyl polysiloxane (VPS) block at varying distances (2.0-, 1.0-, 0.5- and 0.3-mm). Lower illustrations present the implant shoulder was located at the level equal to the surface of VPS block.

implant vertically and transversely in a multiplanar reconstruction view. The cross-sectional image, taken as close as possible through the implant center (Fig. 2a, Line A), was selected and saved so that all examiners would carry out measurements on identical slices (Fig. 3). The contrast and brightness displays of the images were set in advance on a laptop to provide constant viewing settings for the examiners. The VPS thickness next to the micro-thread surface on the CBCT images was recorded at 2-mm level from the top of the implant. The VPS thickness next to the macro-thread surface was recorded at 5-mm level from the top of the implant (Fig. 2b). Two examiners (P.J. K. and C. Y.L.) performed a series of measurements using the obtained images. All measurements were made three times, with an interval of one week between each measurement.

## Preparing ground sections for gold standard measurements (GS)

Following the scanning of the VPS blocks, sections were prepared for direct measurements. A VPS block was infiltrated and fixed on resin using Technovit 7200 VLC (Heraeus Kulzer, Hanau, Germany) embedded in a light-proof container under a vacuum with gentle agitation for a minimum of 1 day. After adequate infiltration, a polymerization process was carried out in a light-polymerizing unit (EXAKT, Remscheid, Germany), initially under low-intensity white light for 6 h and then under high-intensity UV light for a further 2 h. The blocks were then sectioned and cut parallel along the long axis of the implant and according to the line A on CBCT imaging, allowing visualization and later measurement of the VPS thickness. The electronic caliper-measured gold standard measurements of VPS, corresponding to levels examined on the CBCT images, were then carried out using electronic calipers.

## Statistical analysis

All of the collected data were analyzed using a statistical software package (SPSS vers. 15.0, IBM, Chicago, IL, USA). In this study, various measurements were used to describe the VPS width obtained, including GS measurement and the

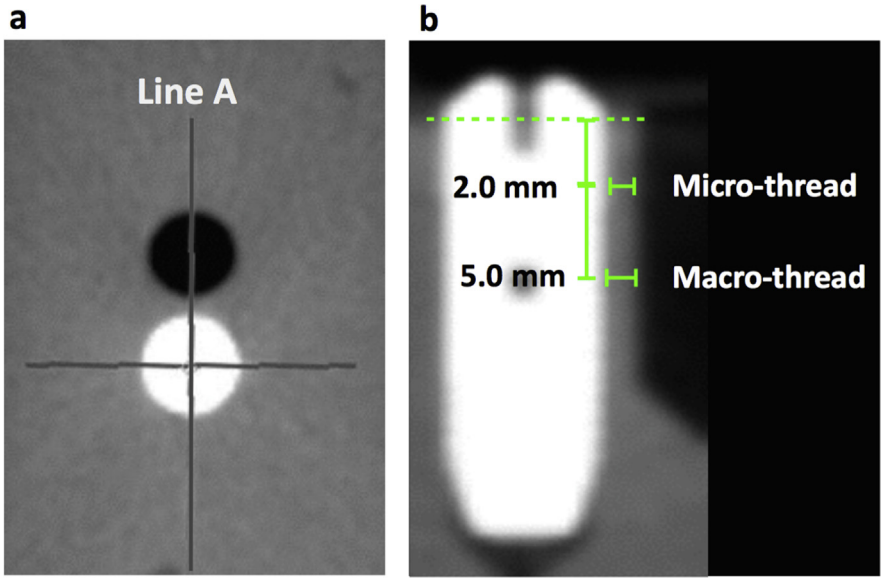


**Figure 2** (a) Example of the axial slice used to identify the reference line A in cone beam computed tomography (CBCT) (b) Example of the sagittal slice selected to measure the VPS thicknesses next to the implant at 2 mm levels (for the micro-thread surface) and 5 mm levels (for the macro-thread surface) from the top of the implant.

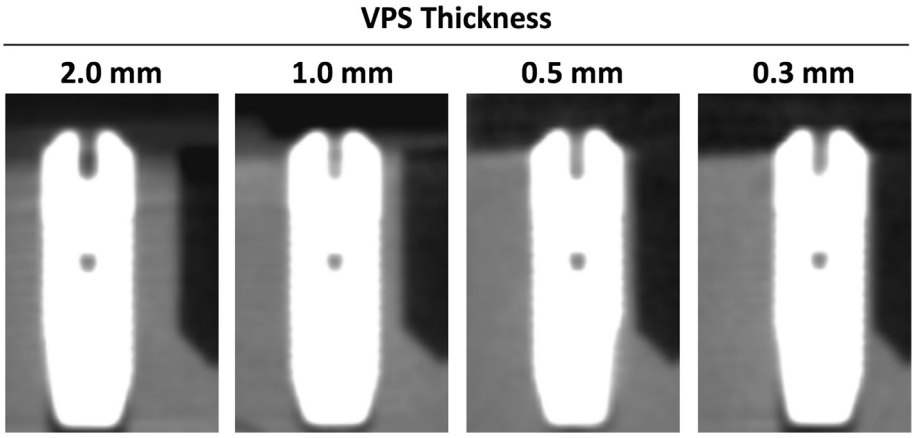


**Figure 3** CBCT sagittal images of four different VPS thicknesses next to the implants.

measured radiographic thickness (RT). The difference and the measured percentage of error between the GS and RT measurements [(GS-RT)/GS × 100%] were also calculated.

Differences between the RT and GS measurements at the different thread designs were compared using a paired *t*-test. All data are expressed as the mean and standard deviation (SD), and $p < 0.05$ was accepted as the significance level. Intra-examiner reproducibility was investigated by examining measurements from two of the implants using the intra-class correlation coefficient (ICC). Inter-examiner agreement was assessed in a similar manner. Reproducibility of each of the GS measurements was analyzed by calculating the coefficient of variation (COV) in percent.

## Results

The COV of measurement for each of the implants at the two measurement levels was calculated, and it was <5%. The overall good reproducibility of the measurements was demonstrated. The range of ICCs for inter-examiner agreement and intra-examiner agreement was 0.82—0.91. This finding demonstrated a high level of agreement between examiners and good reproducibility within examiners.

Results of the mean and SD of CBCT measurements and GS measurements between the two thread designs for each implant are presented in Table 1. The data are shown in graphic form in Fig. 4 and Fig. 5.

The GS measurements were very similar at 2.0- and 5.0-mm levels in groups with different VPS thicknesses (2.0, 1.0, 0.5, and 0.3 mm). However, CBCT-measured thicknesses at the level of micro-thread surface (2.0-mm level) were consistently underestimated compared to GS measurements when the VPS thickness was <2.0 mm (Fig. 4).

In comparison, CBCT measurements at the macro-thread surface (5.0-mm level) closely approximated the GS measurements, except when the VPS thickness was 0.3 mm. When VPS thicknesses were 1.0, 0.5, and 0.3 mm, the CBCT measured thickness dimensions revealed significant differences between two thread systems (Fig. 4).

The mean percentages of errors from the standard measurements in groups with 2.0-, 1.0-, 0.5-, and 0.3-mm thicknesses were 4.8%, 16.4%, 37.8%, and 92.6%, respectively, at micro-thread surface and 0.6%, 2.9%, 9.5%, and 40.8%, respectively, at the macro-thread surface (Fig. 5).

## Discussion

During the design phase and preparation of the methodology, several special cares were taken to minimized the occurrence of tomography technical artifacts in this

**Table 1** Mean (SD) of CBCT measurements and GS measurements and the differences between these two measurements for each VPS thickness group. (Significant differences from the GS: $*P < 0.05$, significant differences from the micro-thread group: $\#P < 0.05$).

| VPS Thickness | Micro-thread | | Macro-thread | |
|---|---|---|---|---|
| | Mean | (SD) | Mean | (SD) |
| Thickness = 2.0 mm | | | | |
| GS | 2.05 | (0.01) | 2.05 | (0.01) |
| CBCT | 1.95 | (0.07) | 2.03 | (0.04) |
| Difference | 0.11 * | (0.08) | 0.01 | (0.03) |
| % of error | 4.77 | | 0.61 | |
| Thickness = 1.0 mm | | | | |
| GS | 1.01 | (0.01) | 1.00 | (0.01) |
| CBCT | 0.85 | (0.06) | 0.96 | (0.04) |
| Difference | 0.17 * | (0.06) | 0.03# | (0.04) |
| % of error | 16.45 | | 2.95 | |
| Thickness = 0.5 mm | | | | |
| GS | 0.54 | (0.02) | 0.54 | (0.01) |
| CBCT | 0.34 | (0.05) | 0.49 | (0.07) |
| Difference | 0.21 * | (0.05) | 0.05# | (0.06) |
| % of error | 37.83 | | 9.53 | |
| Thickness = 0.3 mm | | | | |
| GS | 0.33 | (0.02) | 0.33 | (0.03) |
| CBCT | 0.03 | (0.05) | 0.21 | (0.03) |
| Difference | 0.31 * | (0.04) | 0.14 *,# | (0.03) |
| % of error | 92.65 | | 40.78 | |

CBCT: cone beam computed tomography, GS: electronic calipers measurement as the gold standard, VPS: vinyl polysiloxane.
* Significant differences from the GS, $P < 0.05$.
# Significant differences from the micro-thread group, $P < 0.05$.

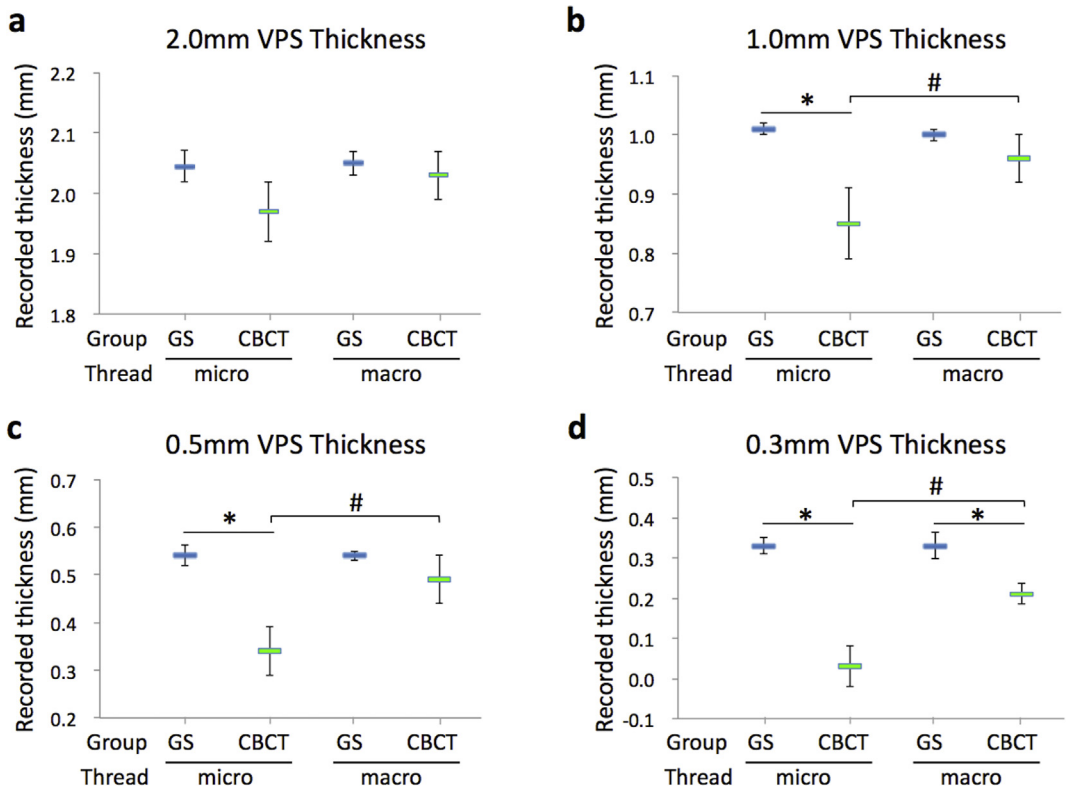


**Figure 4** The graphs present the CBCT measurements and gold-standard (GS) measurements at micro- and macro-thread surface in (a) 2.0-mm, (b) 1.0-mm, (c) 0.5-mm and (d) 0.3-mm VPS thicknesses (Results are presented as mean ± stand deviation (SD). Significant differences from the GS: $*P < 0.05$, significant differences from the micro-thread group: $\#P < 0.05$).

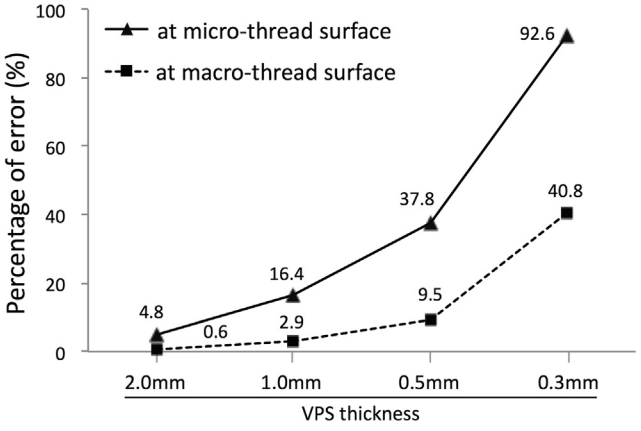


**Figure 5** The graph presents the mean percentage of error (%) at micro- and macro-thread surface in different VPS thickness groups.

present study. However, some artifacts due to the metal dental implant could be observed in the radiographic imaging (Fig. 3). The artifacts were frequently found in axial images of high density structure such as metal material. Numerous studies have focused on beam-hardening artifacts,[11] metallic artifacts,[12] truncated view artifacts,[13] and the image quality of CBCT associated with dental implants.[14] In general, as to measurements of the VPS materials, CBCT underestimated the thicknesses compared to GS measurements (Fig. 4). Moreover, in 0.3 mm VPS thickness group, the examiners had difficulty in visualizing the thickness of head-tissue-mimicking material in CBCT image. This may have been related to beam-hardening artifacts caused by the dental implants.[15] When photons of the x-ray beam pass through an object, low-energy photons are absorbed in preference to higher-energy photons, which results in beam-hardening artifacts in areas with strong x-ray absorption such as metal structures.[16]

Within the radiographic reconstructed image, beam-hardening artifacts manifest as two different artifacts, cupping artifacts and streaks artifacts. The cupping artifacts occur when X-rays that pass through the center of the object become harder than those passing through the edges. The streaks artifacts present as dark streaks or bands between two dense objects, such as two dental implants. These artifacts will change the visibility of hard tissue and result in inaccurate assessment of peri-implant regions.[6,7,17]

As far as we know, this is the first study to compare differences in errors of CBCT images between micro- and macro-thread implant surfaces. Results showed that the mean percentage error increased from measurements at a 2.0-mm VPS thickness to those at thicknesses of 1.0, 0.5, and 0.3 mm. The percentage error was consistently higher at the 2.0-mm measurement level (micro-thread surface group) (Fig. 5). The micro-thread design of implant surfaces will affect the image around the implant, especially when the VPS thickness decreases. When the micro-thread surface implant was measured at a VPD thickness of 0.3 mm, we found an incredible error percentage of 92.6%,

compared to the error found at the macro-thread surface of 40.8%. The difference observed in this study might have resulted from the various degrees of the beam-hardening effect within micro- and macro-threads. The results may be explained by considering the micro-thread surface of implant could enhance the beam-hardening artifact. Moreover, the results of this study were partially supported by previous study, it was concluded that CBCT may not produce sufficient accurate measurement of the thin bone next to the implant. Moreover, they found the CBCT deviating 1.20 mm from the histology regarding bone defects.[7] In the other study, the authors used CBCT to scan the jaws of dogs being treated with dental implants and bone augmentation procedures.[9] They concluded that the evaluation of peri-implant bone defect by means of CBCT is not accurate for sites providing a bone width below 0.5 mm.

In previous study, the authors clam that implant artifacts produced no interference with the measurements, as the implant dimensions were retained in the CBCT.[8] This result probably due to software filters for imaging formatting and the design of the examination. It should be notice that all mean of radiographic measurement distances in that study were >1.0 mm. It is likely that when the targeted object was large enough, according to this present study >1 mm, CBCT technique is reliable for the clinical assessment and provides good accuracy with less measurement error.[18–22] However, the clinical peri-implant bone thickness was usually near 1 mm, and the bone wall could even be thinner when under post-surgical resorption or inflammatory infection. Moreover, one *in vitro* study showed that the CBCT measurements closely approximated the standard, except when the cortical bone thickness was not less than 0.8 mm.[7] A previous animal study demonstrated that the CBCT measurement was not accurate for sites providing a bone wall <0.5 mm next to the dental implant.[9] When the VPS thickness was less 0.3 mm the material possibly too thin to maintain the integrity during sample preparation. Therefore, 0.5 mm and 0.3 mm VPS thickness groups were designed to evaluate the measurement accuracy in this study and we hope the strict design of experiment could answer some clinical problem in the daily practice.

Many materials related to the accuracy of linear measurement have been investigated. Those materials are sufficient to examine superficial anatomical sites and distances.[7,19,22] However, preparing the thin thickness of the sample next to the implant is very difficult and prone to bias under those models. The VPS is one of the elastic impression materials that most commonly used in oral rehabilitation. It has both optimal rigidity and elasticity that could maintain the physical integrity under preparing the different thicknesses of VPS sample adjacent to dental implant especially in 0.5, 0.3 mm thin thicknesses. It also provides sufficiently radiodensity that similar to human dentine and bone.[23] In order to prepare the hard-tissue-mimicking material to simulate the environment of the oral cavity, we created the VPS block *in vitro* model which was much more consistent and homogenous than other materials used in previous studies.[7,19,22] Although it might not completely mimic human hard tissues, it could produce a consistent radiopacity and thin thickness next to the implant with this easily accessible material.

In addition, the effects of voxel size on image resolution have been described.[7,24] Furthermore, the voxel size setting of the CBCT machine was set to 25 μm in this investigation. Any distance measurement might contain an unavoidable error of at least this voxel size. In the depth of micro-thread surface (22 μm) in this present study are charged as potential sources for error, limiting the precision of measurements by blurring the boundaries between hard-tissue-mimicking materials to implant interfaces in CBCT imaging. The similar effect was also observed in the 0.3-mm VPS thickness group, the error percentages were much higher than other VPS thickness groups.

Within the limitations of this study, we conclude that CBCT may not produce sufficient resolution for thin sections of hard tissue-mimicking materials adjacent to dental implants, especially for those near micro-thread design surfaces.

## Conflicts of interest

The authors report no conflicts of interest related to this study.

## Acknowledgements

This study was partially supported by a research grant from Chi Mei Medical Center, Tainan, Taiwan and Taipei Medical University, Taipei, Taiwan (100CM-TMU-11). The implants were kindly supplied by Dentsply.

## Appendix A. Supplementary data

Supplementary data to this article can be found online at https://doi.org/10.1016/j.jds.2019.04.001.

## References

1. Grunder U, Gracis S, Capelli M. Influence of the 3-D bone-to-implant relationship on esthetics. *Int J Periodontics Restor Dent* 2005;25:113–9.
2. Tortamano P, Camargo LO, Bello-Silva MS, Kanashiro LH. Immediate implant placement and restoration in the esthetic zone: a prospective study with 18 months of follow-up. *Int J Oral Maxillofac Implant* 2010;25:345–50.
3. Brief J, Edinger D, Hassfeld S, Eggers G. Accuracy of image-guided implantology. *Clin Oral Implant Res* 2005;16:495–501.
4. Liang X, Jacobs R, Hassan B, et al. A comparative evaluation of Cone Beam Computed Tomography (CBCT) and Multi-Slice CT (MSCT) Part I. On subjective image quality. *Eur J Radiol* 2010;75:265–9.
5. Schulze R, Heil U, Gross D, et al. Artefacts in CBCT: a review. *Dentomaxillofacial Radiol* 2011;40:265–73.
6. Pauwels R, Stamatakis H, Bosmans H, et al. Quantification of metal artifacts on cone beam computed tomography images. *Clin Oral Implant Res* 2013;24(Suppl. A100):94–9.
7. Razavi T, Palmer RM, Davies J, Wilson R, Palmer PJ. Accuracy of measuring the cortical bone thickness adjacent to dental implants using cone beam computed tomography. *Clin Oral Implant Res* 2010;21:718–25.
8. Shiratori LN, Marotti J, Yamanouchi J, Chilvarquer I, Contin I, Tortamano-Neto P. Measurement of buccal bone volume of

dental implants by means of cone-beam computed tomography. *Clin Oral Implant Res* 2012;23:797—804.
9. Fienitz T, Schwarz F, Ritter L, Dreiseidler T, Becker J, Rothamel D. Accuracy of cone beam computed tomography in assessing peri-implant bone defect regeneration: a histologically controlled study in dogs. *Clin Oral Implant Res* 2012;23:882—7.
10. Corpas Ldos S, Jacobs R, Quirynen M, Huang Y, Naert I, Duyck J. Peri-implant bone tissue assessment by comparing the outcome of intra-oral radiograph and cone beam computed tomography analyses to the histological standard. *Clin Oral Implant Res* 2011;22:492—9.
11. Draenert FG, Coppenrath E, Herzog P, Muller S, Mueller-Lisse UG. Beam hardening artefacts occur in dental implant scans with the NewTom cone beam CT but not with the dental 4-row multidetector CT. *Dentomaxillofacial Radiol* 2007;36: 198—203.
12. Zhang Y, Zhang L, Zhu XR, Lee AK, Chambers M, Dong L. Reducing metal artifacts in cone-beam CT images by preprocessing projection data. *Int J Radiat Oncol Biol Phys* 2007; 67:924—32.
13. Mozzo P, Procacci C, Tacconi A, Martini PT, Andreis IA. A new volumetric CT machine for dental imaging based on the cone-beam technique: preliminary results. *Eur Radiol* 1998;8: 1558—64.
14. Loubele M, Van Assche N, Carpentier K, et al. Comparative localized linear accuracy of small-field cone-beam CT and multislice CT for alveolar bone measurements. *Oral Surg Oral Med Oral Pathol Oral Radiol Endod* 2008;105:512—8.
15. Watzke O, Kalender WA. A pragmatic approach to metal artifact reduction in CT: merging of metal artifact reduced images. *Eur Radiol* 2004;14:849—56.
16. Schulze RK, Berndt D, d'Hoedt B. On cone-beam computed tomography artifacts induced by titanium implants. *Clin Oral Implant Res* 2010;21:100—7.
17. Scarfe WC, Farman AG. What is cone-beam CT and how does it work? *Dent Clin N Am* 2008;52:707—30.
18. Agbaje JO, Jacobs R, Maes F, Michiels K, van Steenberghe D. Volumetric analysis of extraction sockets using cone beam computed tomography: a pilot study on ex vivo jaw bone. *J Clin Periodontol* 2007;34:985—90.
19. Kobayashi K, Shimoda S, Nakagawa Y, Yamamoto A. Accuracy in measurement of distance using limited cone-beam computerized tomography. *Int J Oral Maxillofac Implant* 2004;19:228—31.
20. Lund H, Grondahl K, Grondahl HG. Accuracy and precision of linear measurements in cone beam computed tomography Accuitomo tomograms obtained with different reconstruction techniques. *Dentomaxillofacial Radiol* 2009;38:379—86.
21. Loubele M, Guerrero ME, Jacobs R, Suetens P, van Steenberghe D. A comparison of jaw dimensional and quality assessments of bone characteristics with cone-beam CT, spiral tomography, and multi-slice spiral CT. *Int J Oral Maxillofac Implant* 2007;22:446—54.
22. Berco M, Rigali Jr PH, Miner RM, DeLuca S, Anderson NK, Will LA. Accuracy and reliability of linear cephalometric measurements from cone-beam computed tomography scans of a dry human skull. *Am J Orthod Dentofacial Orthop* 2009; 136:17 e1—9.
23. Fonseca RB, Branco CA, Haiter-Neto F, et al. Radiodensity evaluation of dental impression materials in comparison to tooth structures. *J Appl Oral Sci* 2010;18:467—76.
24. Wenzel A, Haiter-Neto F, Frydenberg M, Kirkevang LL. Variable-resolution cone-beam computerized tomography with enhancement filtration compared with intraoral photostimulable phosphor radiography in detection of transverse root fractures in an in vitro model. *Oral Surg Oral Med Oral Pathol Oral Radiol Endod* 2009;108:939—45.